410870

WT-1307 (EX)
EXTRACTED VERSION

OPERATION REDWING

Project 1.8
Crater Measurements

May-July 1956

Pacific Proving Grounds

NOTICE

This is an extract of WT-1307, Operation REDWING, which remains classified SECRET/FORMERLY RESTRICTED DATA as of this date.

BEST COPY AVAILABLE

Extract version prepared for:

Director
DEFENSE NUCLEAR AGENCY
Washington, D.C. 20305

1 January 1981

UNCLASSIFIED

SECURITY CLASSIFICATION OF THIS PAGE (When Data Entered)

REPORT DOCUMENTATION PAGE

READ INSTRUCTIONS BEFORE COMPLETING FORM

1. REPORT NUMBER WT-1307 (EX)	2. GOVT ACCESSION NO.
3. RECIPIENT'S CATALOG NUMBER	
4. TITLE (and Subtitle) Operation REDWING - Project 1.8 Crater Measurements	5. TYPE OF REPORT & PERIOD COVERED
	6. PERFORMING ORG. REPORT NUMBER WT-1307 (EX)
7. AUTHOR(s) J. G. Lewis	8. CONTRACT OR GRANT NUMBER(s)
9. PERFORMING ORGANIZATION NAME AND ADDRESS Headquarters Field Command Armed Forces Special Weapons Project Sandia Base, Albuquerque, N.M.	10. PROGRAM ELEMENT, PROJECT, TASK AREA & WORK UNIT NUMBERS
11. CONTROLLING OFFICE NAME AND ADDRESS	12. REPORT DATE March 12, 1959
	13. NUMBER OF PAGES 37
14. MONITORING AGENCY NAME & ADDRESS (if different from Controlling Office)	15. SECURITY CLASS. (of this report) UNCLASSIFIED
	15a. DECLASSIFICATION/DOWNGRADING SCHEDULE

16. DISTRIBUTION STATEMENT (of this Report)

Approved for public release; unlimited distribution.

17. DISTRIBUTION STATEMENT (of the abstract entered in Block 20, if different from Report)

18. SUPPLEMENTARY NOTES

This report has had the classified information removed and has been republished in unclassified form for public release. This work was performed by the General Electric Company-TEMPO under contract DNA001-79-C-0455 with the close cooperation of the Classification Management Division of the Defense Nuclear Agency.

19. KEY WORDS (Continue on reverse side if necessary and identify by block number)

Operation REDWING
Craters Measurements
Experimental Design

20. ABSTRACT (Continue on reverse side if necessary and identify by block number)

DD FORM 1 JAN 73 1473 EDITION OF 1 NOV 65 IS OBSOLETE

UNCLASSIFIED

SECURITY CLASSIFICATION OF THIS PAGE (When Data Entered)

FOREWORD

This report has had classified material removed in order to make the information available on an unclassified, open publication basis, to any interested parties. This effort to declassify this report has been accomplished specifically to support the Department of Defense Nuclear Test Personnel Review (NTPR) Program. The objective is to facilitate studies of the low levels of radiation received by some individuals during the atmospheric nuclear test program by making as much information as possible available to all interested parties.

The material which has been deleted is all currently classified as Restricted Data or Formerly Restricted Data under the provision of the Atomic Energy Act of 1954, (as amended) or is National Security Information.

This report has been reproduced directly from available copies of the original material. The locations from which material has been deleted is generally obvious by the spacings and "holes" in the text. Thus the context of the material deleted is identified to assist the reader in the determination of whether the deleted information is germane to his study.

It is the belief of the individuals who have participated in preparing this report by deleting the classified material and of the Defense Nuclear Agency that the report accurately portrays the contents of the original and that the deleted material is of little or no significance to studies into the amounts or types of radiation received by any individuals during the atmospheric nuclear test program.

FOREWORD

This report presents the preliminary results of one of the projects participating in the military-effect programs of Operation Redwing. Overall information about this and the other military-effect projects can be obtained from WT-1344, the "Summary Report of the Commander, Task Unit 3." This technical summary includes: (1) tables listing each detonation with its yield, type, environment, meteorological conditions, etc.; (2) maps showing shot locations; (3) discussions of results by programs; (4) summaries of objectives, procedures, results, etc., for all projects; and (5) a listing of project reports for the military-effect programs.

ABSTRACT

The objective of this project was to measure the physical characteristics of craters produced by the detonation of nuclear devices so as to obtain a more thorough understanding of crater-prediction phenomenology.

Crater measurements were made on the five surface or near-surface shots: Lacrosse, Zuni, Seminole, Mohawk, and Tewa. Crater radius, crater depth, and approximate profile were determined by use of aerial photography and lead-line sounding techniques. Aerial mapping photographs were made of the craters after the shots, and these were used to plot ground elevations to give the crater radius. Lead-line soundings were made along diameter(s) of each crater to determine the depth and average profile. The results are summarized in Table 3.1.

PREFACE

The authors gratefully acknowledge the assistance given by the chief and various members of the Special Projects Branch of the U. S. Army Engineer Research and Development Laboratories for their assistance throughout the planning and operational phases of the program; Major H. T. Bingham and LCDR J. F. Clarke, Jr., of Programs 1 and 3, for their assistance during all phases of the test; Lt. Colonel J. G. James and his staff for the aerial photography; Lt. Colonel W. A. Mowery, J-6, for his assistance in establishing the operational requirements for Holmes and Narver; Holmes and Narver personnel who made the preshot and postshot surveys; personnel of Project 5.6, including Floyd Gibbs and staff, Hastings-Raydist, Inc., for recording by Raydist the position of the boat while making the lead-line soundings for the Zuni crater; James W. Halbrook and Ivan R. Jarrett, Map Compilation Branch, U. S. Army Engineer Research and Development Laboratories, for making photogrammetric measurements from the aerial photographs; and Lt. Colonel E. E. Pickering and his staff of Blast Branch, AFSWP, for numerous suggestions throughout the program.

CONTENTS

TABLES

FIGURES

Chapter 1
INTRODUCTION

1.1 OBJECTIVE

The objective of this project was to measure the physical characteristics (radius, depth, and average profile) of craters produced by nuclear detonations. Data were gathered from Shots Lacrosse, Zuni, Seminole, Mohawk, and Tewa. Although all were termed "surface" bursts, the burst elevations actually varied between a 300-foot tower to what may be considered a subsurface burst. It was a further objective of this project to correlate the data obtained with results from previous "surface" bursts at the Eniwetok Proving Ground (EPG) and pertinent TM 23-200 curves.

1.2 BACKGROUND

Measurements of the apparent crater radius and depth for surface shots at the EPG had been made during Operations Greenhouse, Ivy, and Castle (References 1, 2, and 3). Aerial photography techniques were used in these instances to obtain data on crater radius, and fathometer techniques were used during Castle to obtain depth measurements. Since these operations, no new techniques have been developed for the more-refined measurement of crater characteristics, even though more-accurate determination of the depth and profile of a water-filled crater is desirable. The aerial-mapping technique provides ample accuracy for the determination of the crater radius, since it provides data at early times after the burst, when the contamination from radioactive fallout is extremely high.

Project personnel of the U. S. Army Engineer Research and Development Laboratories (USAERDL), Fort Belvoir, Virginia, were successful in making early time measurements on the crater of Shot 7, Operation Teapot. Subsequent to that, Headquarters, Armed Forces Special Weapons Project (AFSWP), requested that USAERDL submit a project proposal for Operation Redwing to accomplish the previously outlined objectives.

1.3 THEORY

In an operation such as Redwing, where the land area available for detonation of large-yield surface bursts is small, compared with the predictable crater size, the extent of the measurements obtainable and an understanding of their physical significance and reliability need considerable clarification. The "apparent crater" is that which is visible to the eye subsequent to the completion of dynamic effects of the explosion, such as throwout and fallout. Such a definition is not readily applicable to the geologic condition encountered at EPG. If the sides of the crater break through to open water, considerable washing by wave action will alter the shape of the apparent crater as strictly defined. This effect would not be important, if it were desired only to compare these shots with others having the same general geologic conditions. This washing action would then take on a similar role to throwout or fallout in defining the phenomena. It would be highly desirable to separate the water-actuated effects from the direct blast-produced crater, but this capability is not yet a reality. Considering the operational difficulties of obtaining early-time crater measurements, a realistic approach would compare craters only when the ground or groundwater conditions are similar and include such induced phenomena as washing action into the definition of the apparent crater, since this induced effect is properly a part of the immediate recovery problem. The water-actuated effects are then a part of the weapon effects for these burst conditions. However, these effects complicate the correlation, scaling, or complete understanding of cratering phenomena from a technical point of view.

Several other factors affect the analysis of data obtained during this project and correlation with data obtained in the past. Ideally speaking, four variables determine the size of the crater from a near-surface detonation of an explosive charge. These are total blast yield, height above or depth below the air-earth interface, energy partition, and soil type. Knowing the relationships of these variables, the volume of a crater and the ratio of its radius to its depth should be calculable.

For a nuclear surface burst, the portion of the hydrodynamic yield that manifests itself in cratering and ground shock can be evaluated on a TNT-equivalent basis by considering the ratio

$$\frac{\text{Weight of TNT required to produce a given crater dimension}}{\text{Hydrodynamic yield to produce the same crater dimension.}}$$

The use of the TNT equivalent allows high-explosive cratering data to be converted into prediction curves for nuclear weapons.

A drawback to this method is the fact that there is little high-explosive data for comparison, both from the point of view of soil type found at the EPG and the high yields necessary for direct comparison.

Griggs (Reference 4) predicted for the Operation Jangle surface shot with good accuracy, calculating that only about 2 percent of the total energy release will go into the ground for a nuclear detonation on an air-ground planar interface. Other estimates by Porzel (Reference 1) indicate about 0.1 percent for EPG soil and 0.6 percent for the more porous Nevada Test Site (NTS) soil. The saturated soil at the EPG cannot be expected to absorb and transmit energy in the same manner as the NTS soil with its high air content (about 40 percent by volume). The NTS soil will react plastically, whereas the saturated soil at the EPG is considered essentially incompressible.

1.4 MILITARY SIGNIFICANCE

Craters from nuclear explosions can be an extremely important weapon effect. There are certain target types, both surface and subsurface, that require a contact (i.e., a cratering) burst to cause significant damage. Massive concrete fortifications, underground structures, heavy industrial machinery, airfield runways, tunnels, and dams are good examples of this type of target. Probably just as important, tactically speaking, is the ability to achieve delaying action to an enemy by the use of craters, crater lips, and their high residual contamination as barriers.

If a crater is to be used as an obstacle, or part of a barrier system, its effectiveness is dependent upon the ratio of its radius to depth or the slope of its sides. Previous data indicate that for a surface burst as the yield increases so does this ratio, and as the depth of burst increases this ratio decreases. However, the crater is more effective as an obstacle to vehicular movement when this ratio is small and the slope of the sides steep.

It is felt that too much weight should not be placed on the nonconformity of individual craters formed from tower bursts, since these are depression craters formed in the high-overpressure region of the burst. The outer limits of these craters are very hard to detect, except by very-accurate survey controls. This is particularly true when one realizes that the radius-to-depth ratio of the crater being considered may be on the order of 100.

In order for a military commander to properly use the cratering effect from a nuclear weapon and still execute tactical operations on the ground, he must have an understanding of the variation in crater dimensions due to the burst position of the weapon (above or below the air-earth interface), placement of the weapon (tamped or untamped), yield of the weapon, and response of the media in the vicinity of the detonation.

Chapter 2
EXPERIMENTAL DESIGN

2.1 AERIAL PHOTOGRAPHY

Aerial photographs were taken of each of the five shot areas (Lacrosse, Zuni, Seminole, Mohawk, and Tewa), so the apparent diameter of the crater could be measured photogrammetrically. Exposed crater contours were also determined by the same means. An RB-50E aircraft equipped with a USAF aerial mapping camera, T-11, having a 6-inch focal length, was used to make the mapping runs. The camera was gyrostabilized and the intervalometer was set for a forward overlap of 57 to 62 percent. Calibration certificates are on file at USAERDL for all T-11 cameras, thus precluding the necessity for special calibration runs. Film was developed at EPG to insure proper coverage of the target and then sent to Fort Belvoir for analysis.

Readings of a radio altimeter, FCR 718, were taken at the beginning of each mapping run and any variations were noted. This instrument can indicate the altitude above the surface of the ground between 200 and 60,000 feet with an accuracy of ± 25 feet over smooth terrain. The flight pattern was flown as soon after the shot as possible (approximately H + 2 to H + 32 hours).

Photogrammetric measurements were made at USAERDL. The accuracy of the stereoplotting equipment is limited by the deviation of the altimeter reading from the true value, since the error of the equipment is negligible by comparison.

2.2 DEPTH SOUNDINGS

Lead-line soundings were taken to determine the depth of the apparent crater below the water surface. The time at which these soundings were taken was dependent upon the time required for the site radiation level to decay to a value such that the total exposure of the survey group would not amount to an important fraction of the total allowable dose for the entire operation, viz., 3,900 mr.

2.2.1 Lacrosse. For early preliminary results, a sounding was taken from a helicopter positioned over apparent ground zero approximately 25 feet above the water surface. The sounding was later checked against those taken from a boat and found to be in agreement within 1 foot. When residual radiation was low enough, a survey crew of Holmes and Narver entered and re-established a diameter that had been used in the preshot survey and, using a skiff, made detailed soundings. Because of the symmetry indicated by postshot photography, it was determined that detailed soundings along one diameter would be sufficient.

2.2.2 Zuni. Because of the extensive breaching of the crater, the radiation level was low enough to make re-entry possible at an earlier time than other shots. On D + 6, a survey crew of Holmes and Narver went into the area and made soundings along the presurveyed diameters. The craft used was an LCM, and its position at the time the soundings were made was determined by Raydist.

The use of Raydist to establish the horizontal control location of the lead-line soundings had been previously planned to preclude the need for postsurvey personnel to land on Site Tare to accomplish the horizontal control by conventional survey triangulation methods. The Raydist equipment was already available, because of other Project 5.6 aircraft-tracing requirements. It was considered that the elimination of the need of survey personnel to land on Tare, with its expected relatively high postshot radiological contamination, would permit an earlier crater-depth survey by at least several days. Because of the rather severe postshot tidal-wash action expected through the Zuni crater area, which would possibly modify the initial crater measurements considerably, it was obviously desirable that the postshot lead-line soundings be made as soon as possible after the shot.

The position of ground zero was determined before shot time by Raydist, and the LCM craft was guided to this spot for the beginning of each run along the radii. The course of the craft along these radii was governed by compass direction.

2.2.3 Seminole, Mohawk, and Tewa. Residual radiation was too high for detailed soundings to be made of these craters while the operation was in progress. Soundings were taken from a helicopter at ground zero for Seminole and Mohawk and reported in the preliminary report. Lead-line soundings made by Holmes and Narver in September and October 1956 are reported in Chapter 3 of this report.

Chapter 3
RESULTS

The results of the crater surveys are summarized in Table 3.1.

3.1 LACROSSE

Figure 3.1 is a preshot photograph of the Lacrosse area. Figure 3.2 is a postshot photograph of the same area; on this photo, line A-B has been drawn to represent the track the survey boat followed while making the lead-line soundings. The results of the preshot and postshot surveys are presented in Figure 3.3. On this and all other profiles, zero elevation has been taken as the datum plane on which tide tables are based: 0.5 feet below mean-low-water spring. Figure 3.4 depicts the contours of the crater determined by photogrammetry.

3.2 ZUNI

Figure 3.5 is a preshot and Figure 3.6 is a postshot photograph of the Zuni area. Figure 3.7 depicts the contour of the crater area as found by photogrammetry measurements. Rays 1, 2, 3, 4, 5, and 6 represent the rays of the preshot survey; Table 3.2 gives the findings in tabular form. Lines A-A′, B-B′, C-C′, D-D′, E-E′, F-F′, and G-G′ represent the track the survey boat followed while making the lead-line soundings; and Table 3.3 gives the findings in tabular form. Figure 3.8 is a plot of depth measurements versus distance from ground zero. The basic data have been corrected to indicate the distance below the datum plane. The curve was drawn as a representative profile of the crater.

3.3 SEMINOLE

Figures 3.9 and 3.10 are the preshot and postshot photographs of the Seminole area. Figure 3.11 depicts the contour of the crater area as found by photogrammetry measurements. Figure 3.12 represents the preshot and postshot survey rays. Figure 3.13 presents profiles of the preshot survey and postshot lead-line soundings.

The device position and surroundings for Seminole require explanation, because it is felt that they had considerable influence on the resultant crater. The nuclear device was placed in a 15-foot-diameter tank, which was itself inside a 50-foot-diameter tank of water. A sketch of this is shown in Figure 3.14. The effects of this tank of water are largely dependent on its size relative to the size of the isothermal sphere in water at hydrodynamic separation. It seems, as will be discussed in Chapter 4, that the tank was sufficiently large for the yield of the Seminole device to go from radiative transport to shock before the isothermal sphere reached the outside of the tank. It is possible that this would affect the crater in two ways: (1) better coupling of energy to the soil and (2) a nonsymmetrical

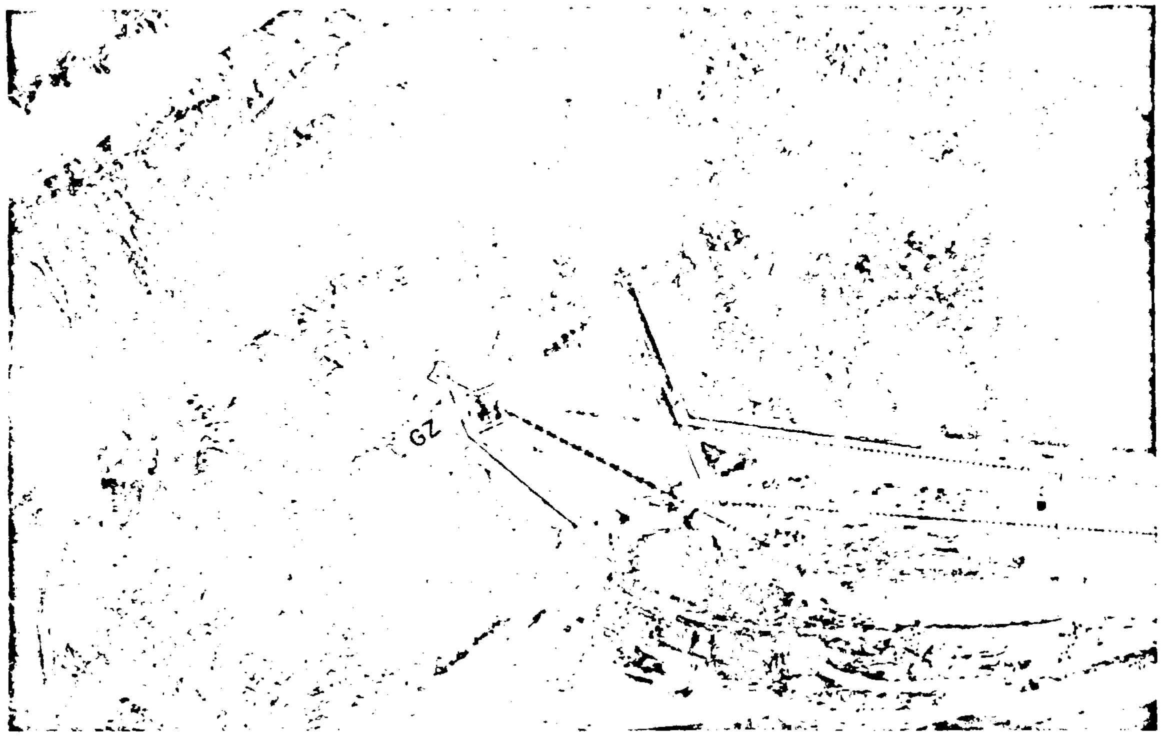

Figure 3.1 Lacrosse, preshot.

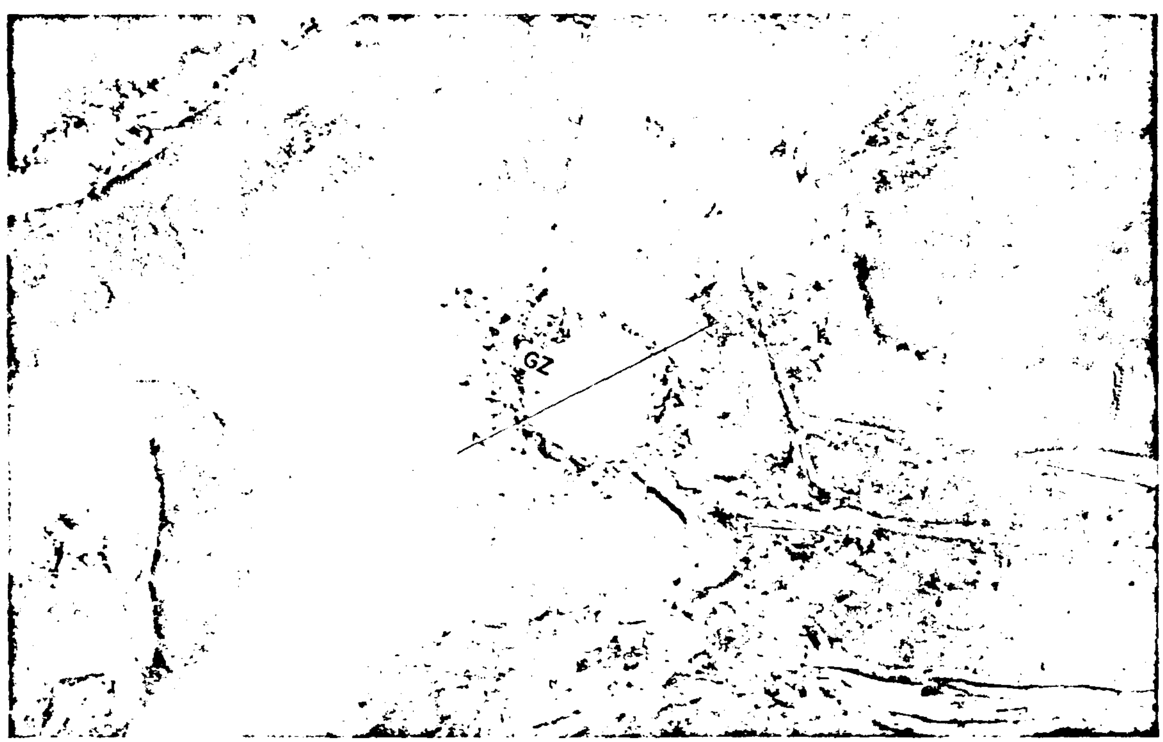

Figure 3.2 Lacrosse, postshot.

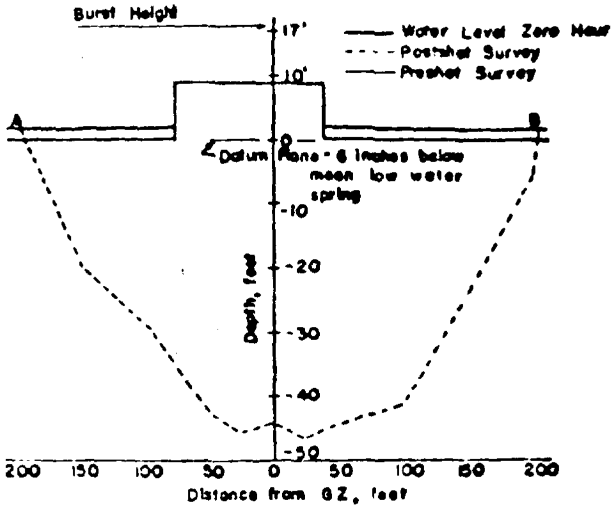

Figure 3.3 Results of Lacrosse lead-line soundings.

crater shape about ground zero. The latter would be caused by the burst point not being in the geometric center of the water tank. Both of these assumptions are supported by the results.

3.4 MOHAWK

Figures 3.15 and 3.16 are the preshot and postshot photographs of the Mohawk area. Figure 3.17 depicts the contour of the crater area as found by photogrammetry measurements. Figure 3.18 shows the postshot survey rays the boat followed while making the lead-line soundings. Figure 3.19 presents profiles of the preshot survey and postshot rod soundings.

3.5 TEWA

Figure 3.20 is a postshot photograph of Tewa. Figure 3.21 shows the postshot lead-line soundings and the course followed by the boat when making these soundings. Both pre-shot and postshot profiles are plotted in Figure 3.22. The preshot survey lines are shown on this figure.

TABLE 3.1 RESULTS OF CRATER SURVEY

Shot	Yield	Height of Burst		Crater Radius		Crater Depth	
		ft*	λ†	ft	λ‡	ft	λ§
Lacrosse	39.5 kt	17	5.00	[illegible]	[illegible]	[illegible]	17.6
Zuni	3.53 Mt	[illegible]	0.61	[illegible]	[illegible]	[illegible]	13.4
Seminole		−12¶		[illegible]		[illegible]	
Mohawk		[illegible]		[illegible]		[illegible]	
Tewa	5.01 Mt	[illegible]	1.17	2,000	117	[illegible]	18.7

* Above mean-low-water spring.
† Height of burst scaled to 1 kt using cube-root scaling.
‡ Crater radius scaled to 1 kt using cube-root scaling.
§ Crater depth scaled to 1 kt using fourth-root scaling.
¶ Adjusted height of burst (see discussion).

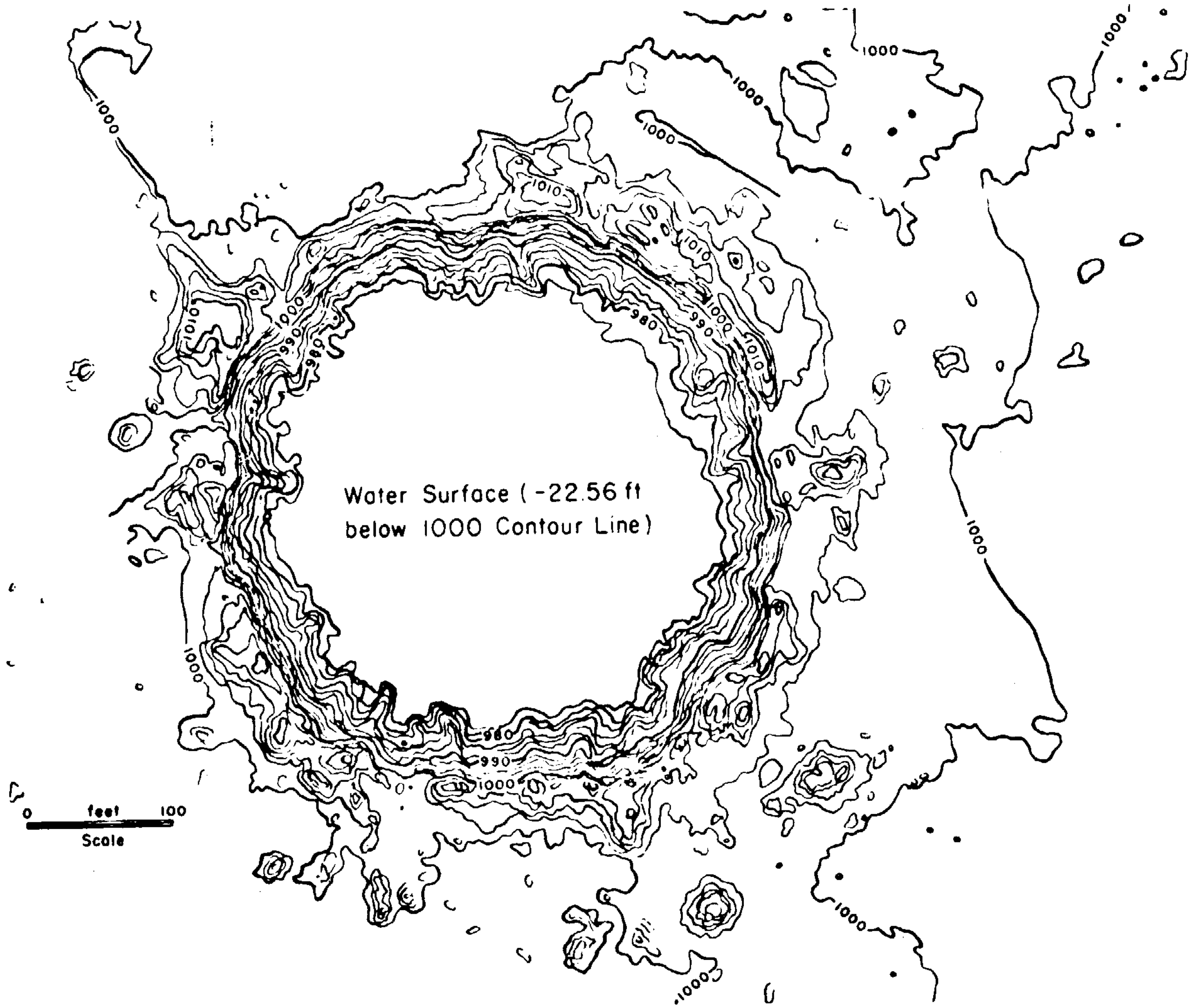

Figure 3.4 Lacrosse stereophotogrammetric measurements; 1,000 contour line is 2.5 feet above the datum plane.

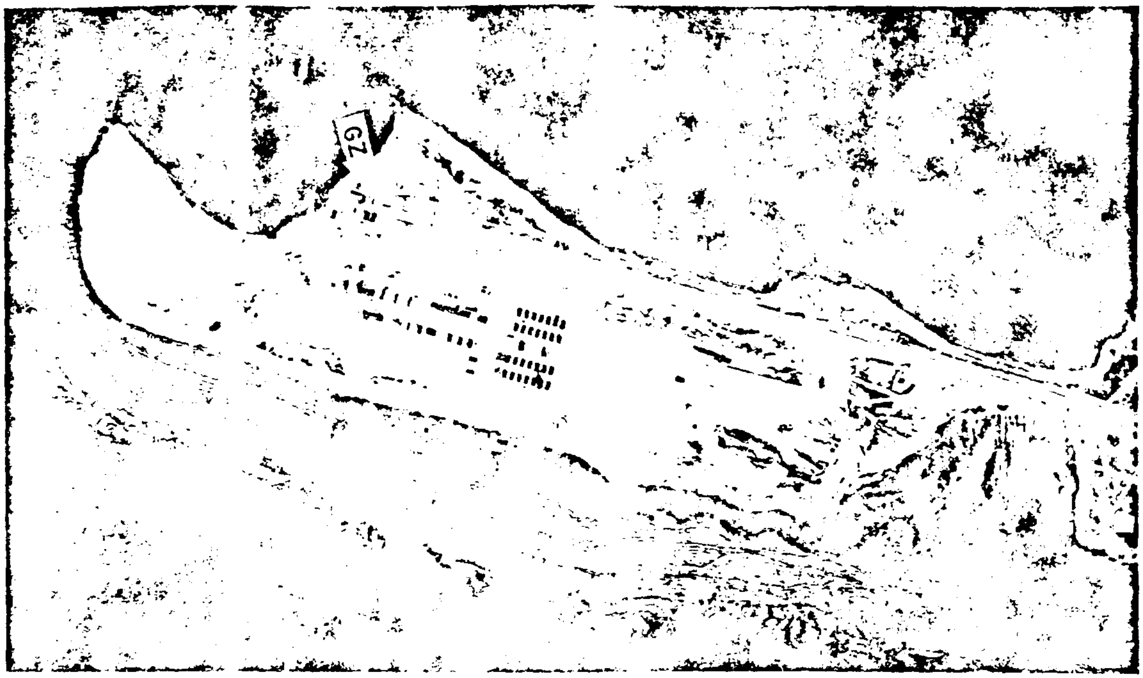

Figure 3.5 Zuni, preshot.

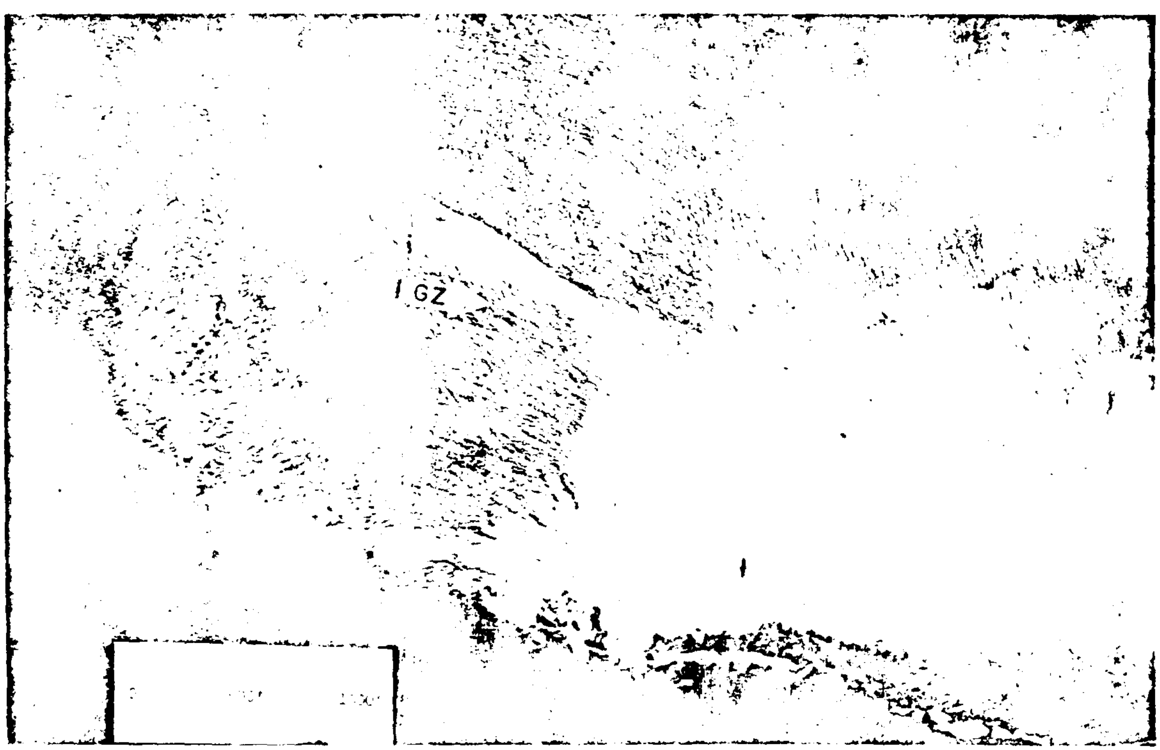

Figure 3.6 Zuni, postshot.

TABLE 3.2 ZUNI PRESHOT SURVEY

Ray	Distance from Ground Zero	Elevation above Datum Plane	Ray	Distance from Ground Zero	Elevation above Datum Plane	Ray	Distance from Ground Zero	Elevation above Datum Plane
	feet	feet		feet	feet		feet	feet
1	0	8.0	3	0	8.0	5	0	8.0
	40	6.4		40	6.4		40	9.6
	100	8.6		115	6.9		100	10.1
	200	11.3		140	7.0		102	3.0
	300	10.5		161	9.7		200	−4.5
	400	10.1		200	10.9		300	−5.0
	500	9.2		300	13.8		400	−5.0
							500	−10.5
	600	8.6		400	13.6			
	700	7.8		500	13.5		626	−16.0
	800	6.9		600	12.8		728	−17.0
	900	7.0		700	10.0		832	−19.0
	1,000	7.5		763	9.5		936	−27.0
	1,100	8.5		778	5.9		1,040	−30.0
	1,200	8.7		800	2.9		1,090	−64.0
							1,144	−86.0
	1,300	8.5		807	1.7		1,248	−102.0
	1,400	8.4		900	0.5			
	1,500	8.5		1,000	0.5		1,352	−108.0
	1,600	8.5		1,100	0.3		1,450	−110.0
	1,700	8.5		1,200	0.0		1,560	−132.0
	1,800	8.6		1,300	0.9		1,670	−168.0
				1,305	0.9		1,768	−170.0
2	0	8.0					1,872	−156.0
	40	6.4	4	0	8.0		1,980	−150.0
	115	7.9		40	6.7			
	140	8.3		90	7.9	6	0	8.0
	155	13.3		98	8.2		115	9.1
	200	14.1		100	3.88		200	9.7
	300	14.9		200	−15.0		300	10.2
	400	14.7		300	−21.1		380	9.8
				405	−24.0		400	6.2
	500	13.2					429	2.9
	600	11.7		500	−23.0			
	700	10.6		600	−22.0		500	−7.0
	752	4.5		700	−23.0		600	−8.0
	800	7.3		825	−10.0		700	−11.0
	822	9.1		935	−7.0		800	−20.0
	865	7.3		980	−0.0		900	−25.0
	873	2.8		1,040	1.0		1,000	−39.0
				1,100	−3.0		1,100	−60.0
	900	2.3						
	1,000	2.1		1,200	−7.1		1,200	−84.0
	1,100	2.2		1,300	−10.5		1,300	−90.0
	1,200	1.2		1,400	−44.0		1,436	−96.0
	1,300	1.2		1,560	−56.0		1,500	−100.0
	1,400	1.1		1,664	−58.0		1,600	−98.0
	1,500	1.1		1,768	−78.0		1,700	−102.0
	1,600	1.2		1,872	−120.0		1,800	−104.0
				2,000	−132.0			

TABLE 3.3 ZUNI, LEAD-LINE SOUNDINGS

Run	Point	Depth	Radial Distance from Ground Zero	Holmes & Narver Coordinates East	North
		feet	feet		
A-A′	1	63	380	110,024	99,912
	2	76	293	110,147	99,954
	3	81	330	110,043	99,967
	4	72	360	109,986	99,987
	5	67	406	109,919	100,044
	6	60	583	109,729	100,123
	7	52	740	109,572	100,167
	8	21	970	109,340	100,193
	9	9	1,087	109,224	100,212
	10	13	1,170	109,141	100,243
B-B′	1	69	183	110,317	99,973
	2	58	287	110,446	99,910
	3	56	387	110,590	99,888
	4	47	540	110,735	99,836
	5	37	657	110,841	99,773
	6	27	687	110,875	99,773
	7	18	720	110,906	99,756
	8	12	753	110,965	99,787
C-C′	1	60	187	110,311	99,975
	2	75	253	110,099	100,010
	3	72	326	109,985	100,175
	4	71	440	109,882	100,281
	5	64	627	109,734	100,429
	6	60	833	109,585	100,574
	7	39	1,063	109,448	100,782
	8	70	1,383	109,222	101,017
D-D′	1	67	267	110,296	99,888
	2	58	513	110,295	99,640
	3	37	753	110,262	99,406
	4	20	863	110,169	99,306
	5	9	1,023	110,055	99,182
E-E′	1	65	273	110,285	99,884
	2	64	140	110,336	100,019
	3	90	50	110,328	100,202
	4	105	217	110,313	100,372
	5	90	337	110,258	100,493
	6	91	487	110,010	100,543
F-F′	1	65	187	110,311	99,975
	2	63	526	110,116	99,664
	3	35	790	109,867	99,500
	4	6	1,073	109,643	99,313
	5	1	1,207	109,513	99,250
G-G′	1	16	1,217	109,103	100,314
	2	10	1,083	109,233	100,285
	3	55	830	109,481	100,210
	4	58	567	109,742	100,170
	5	104	177	110,140	100,212
	6	104	120	110,353	100,278
	7	58	350	110,646	100,235
	8	51	730	111,000	100,226
	9	24	920	111,224	100,221
	10	2	1,033	111,338	100,251

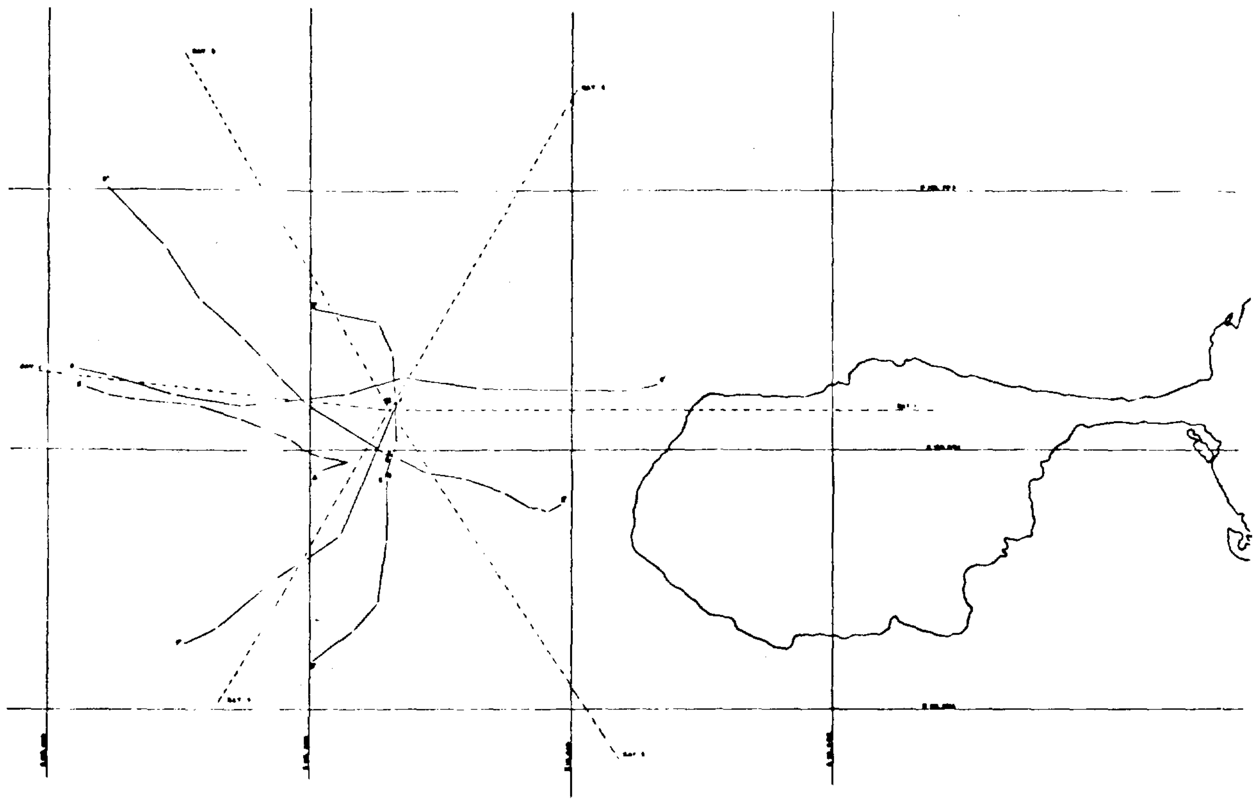

Figure 3.7 Zuni stereophotogrammetric measurements.

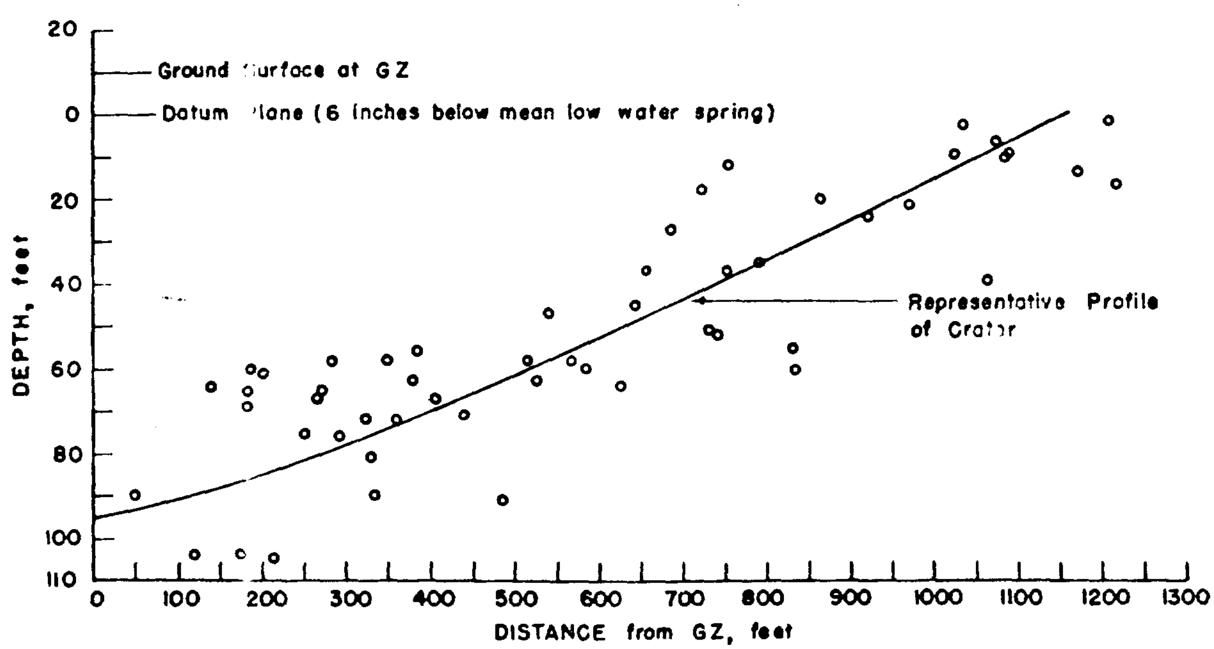

Figure 3.8 Zuni crater profile.

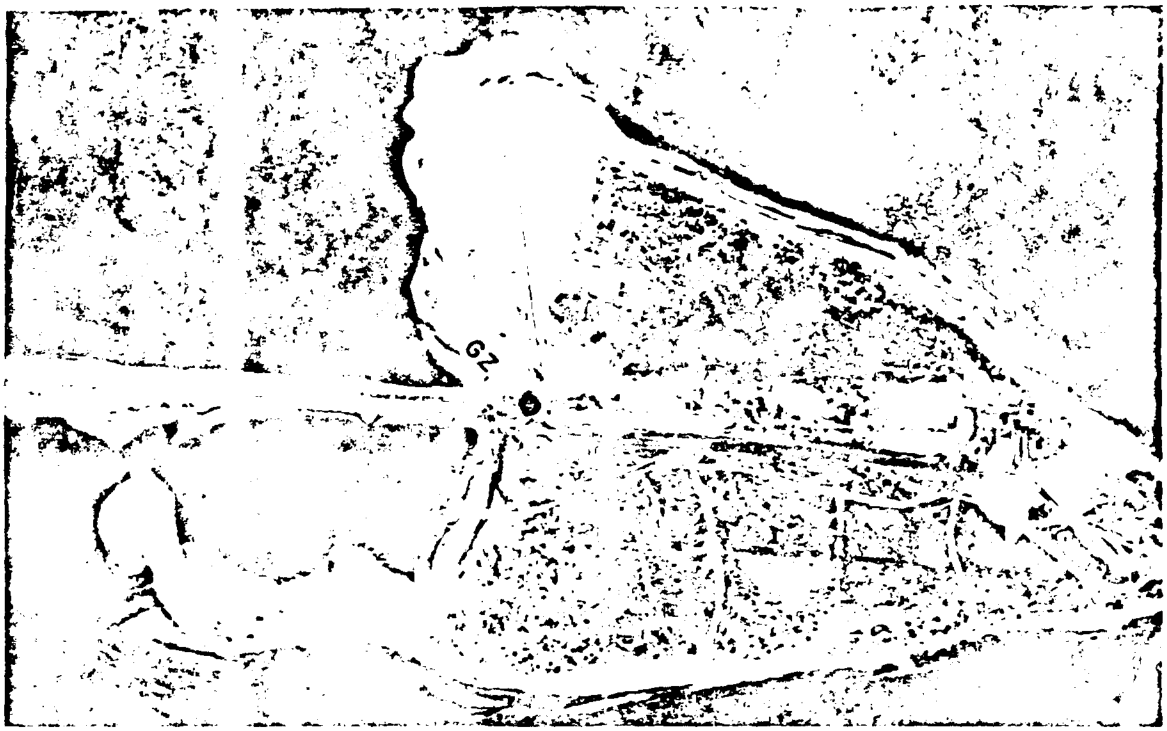

Figure 3.9 Seminole, preshot.

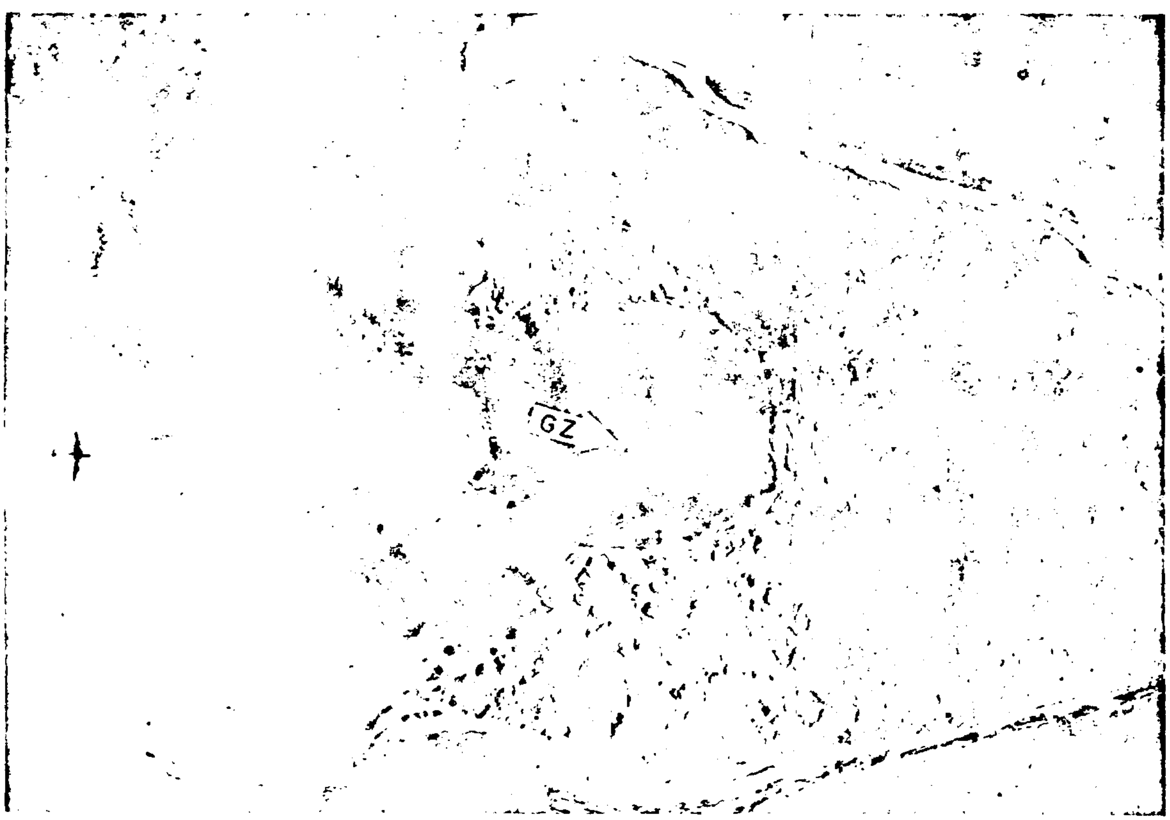

Figure 3.10 Seminole, postshot.

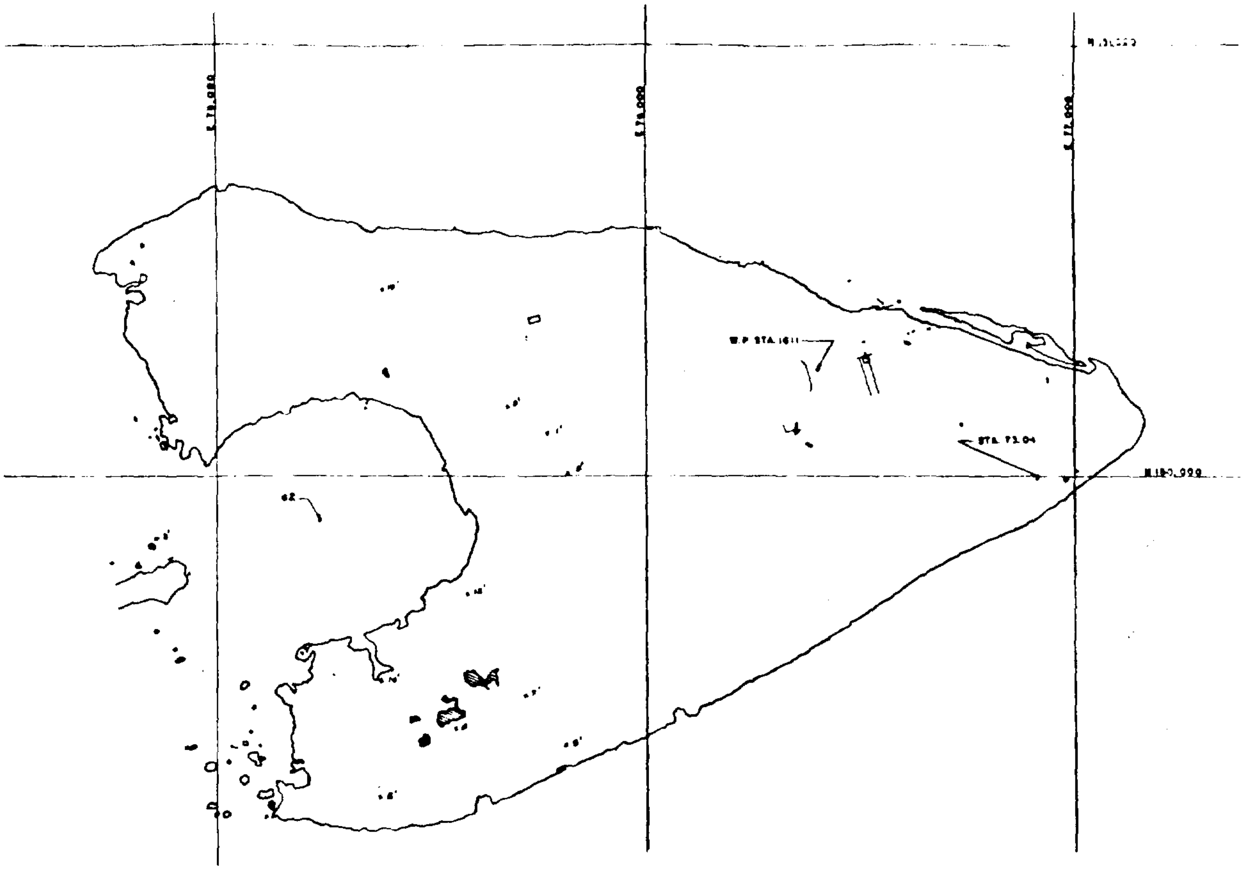

Figure 3.11 Seminole stereophotogrammetric measurements.

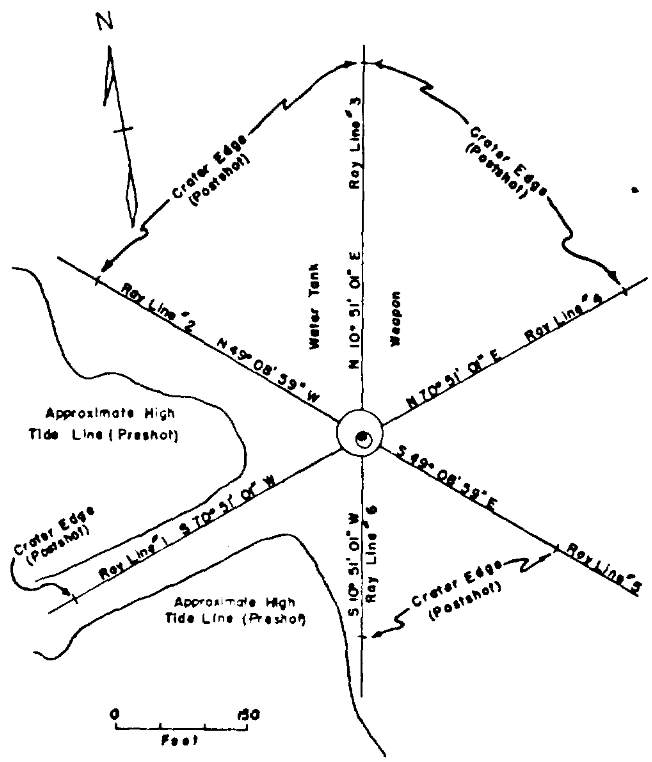

Figure 3.12 Seminole survey lines.

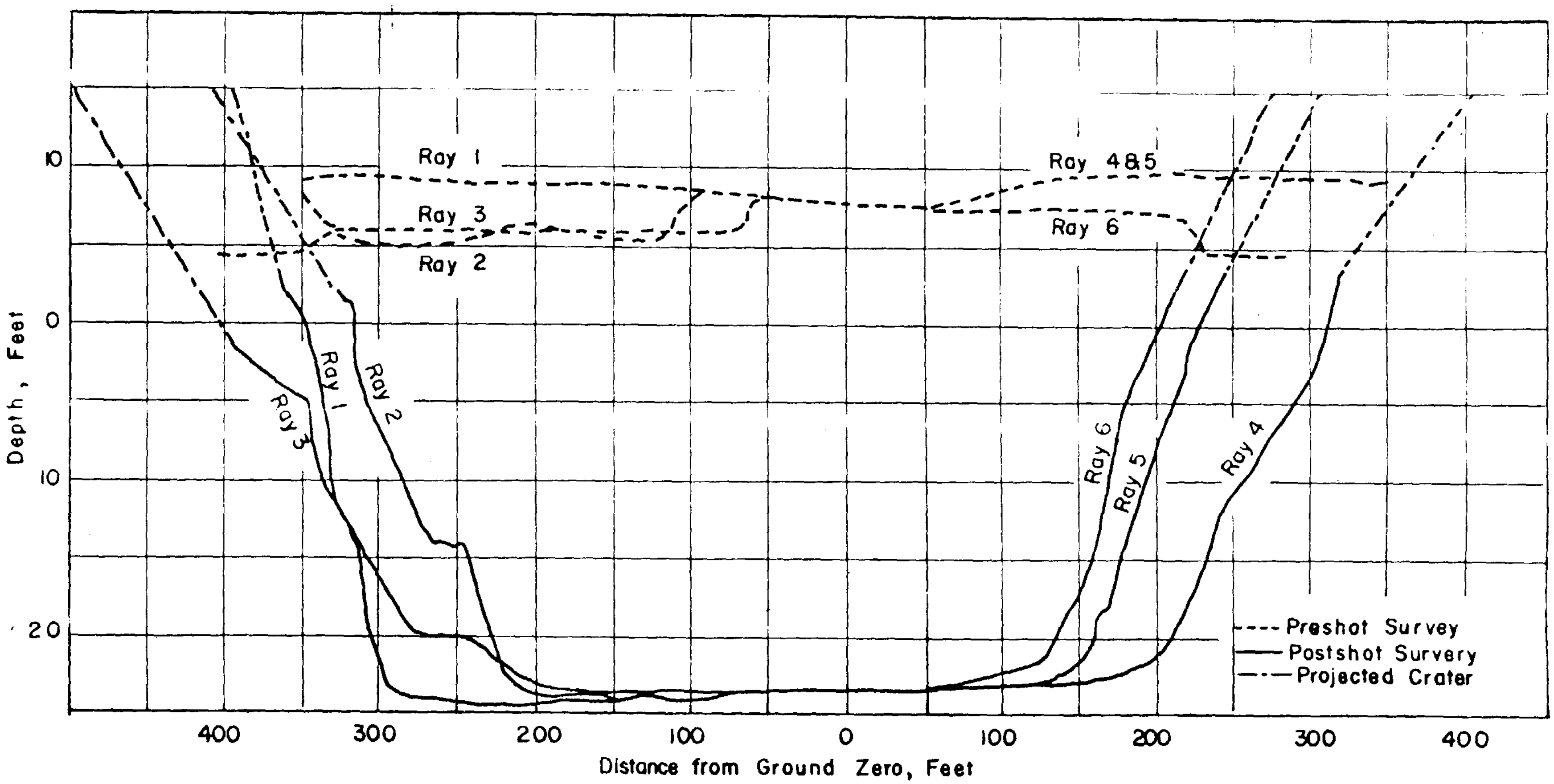

Figure 3.13 Seminole preshot and postshot profiles.

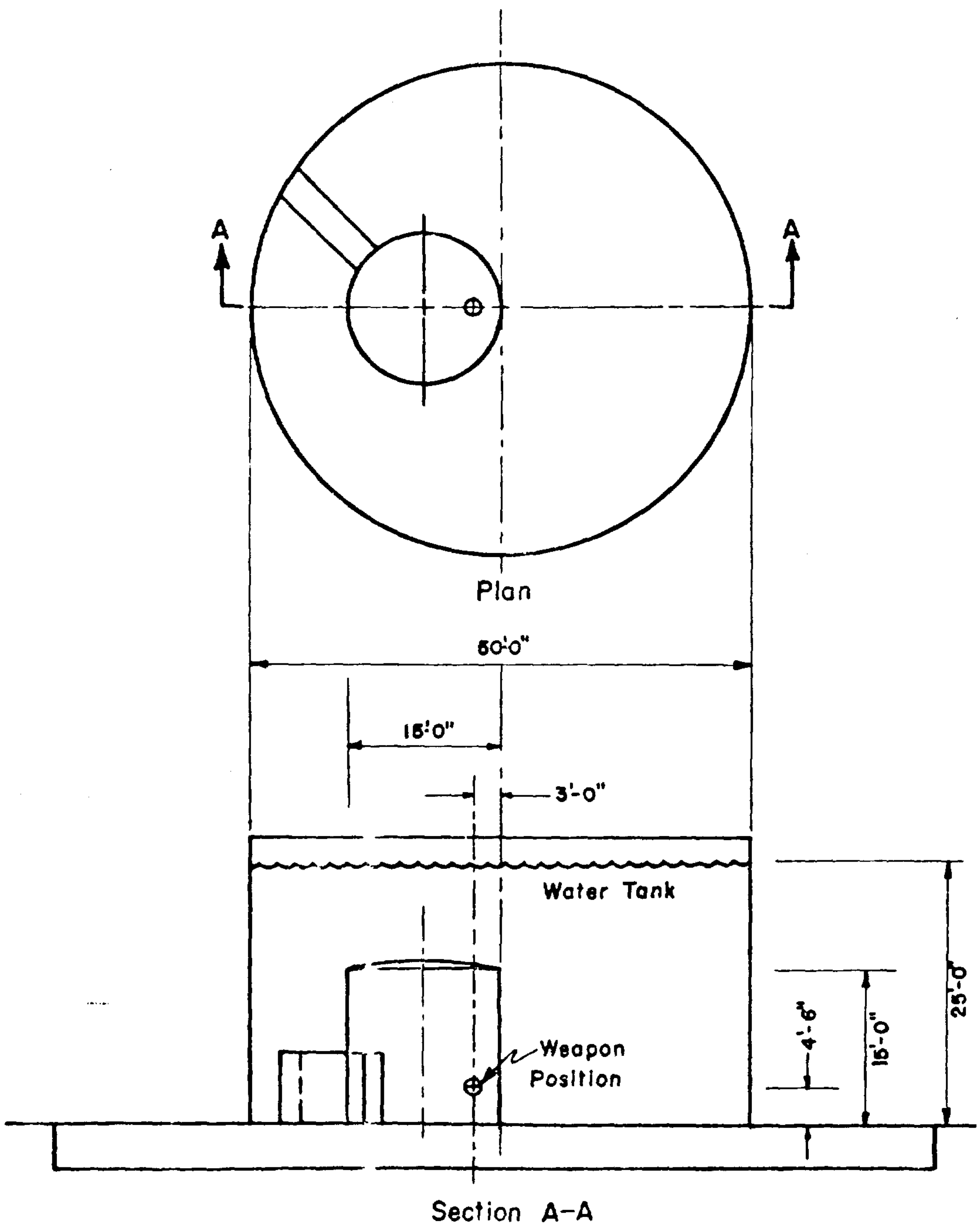

Figure 3.14 Seminole burst position.

Figure 3.15 Mohawk, preshot.

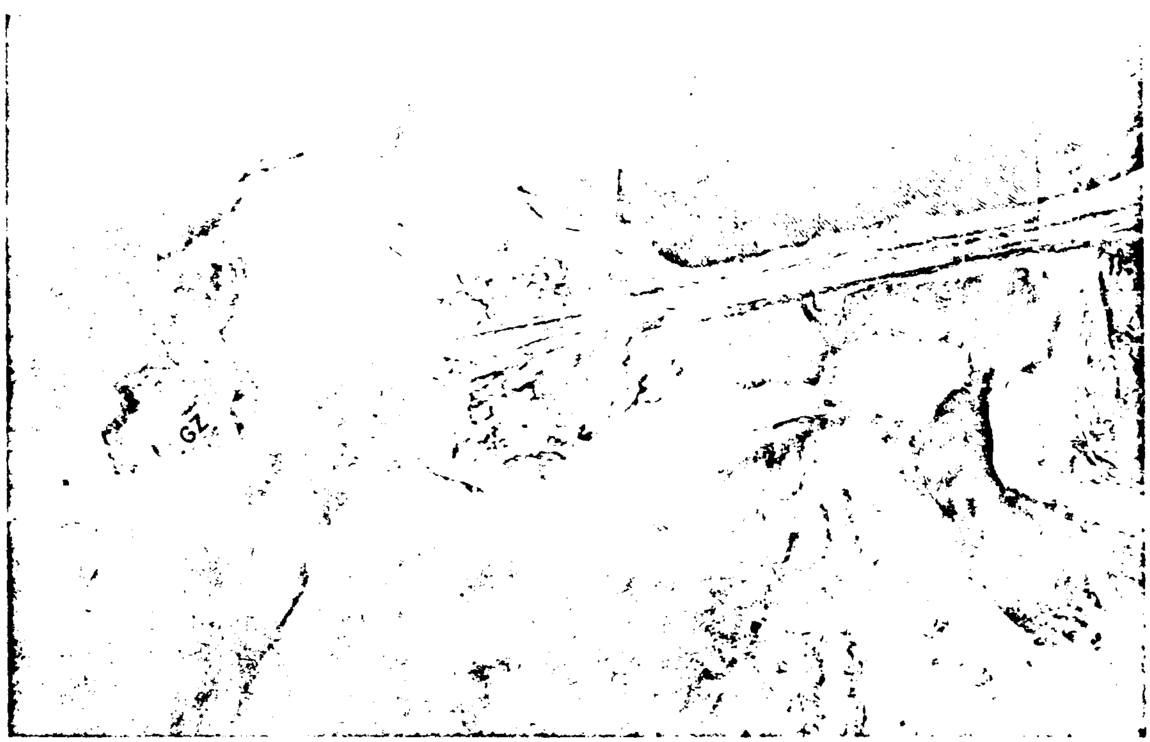

Figure 3.16 Mohawk, postshot.

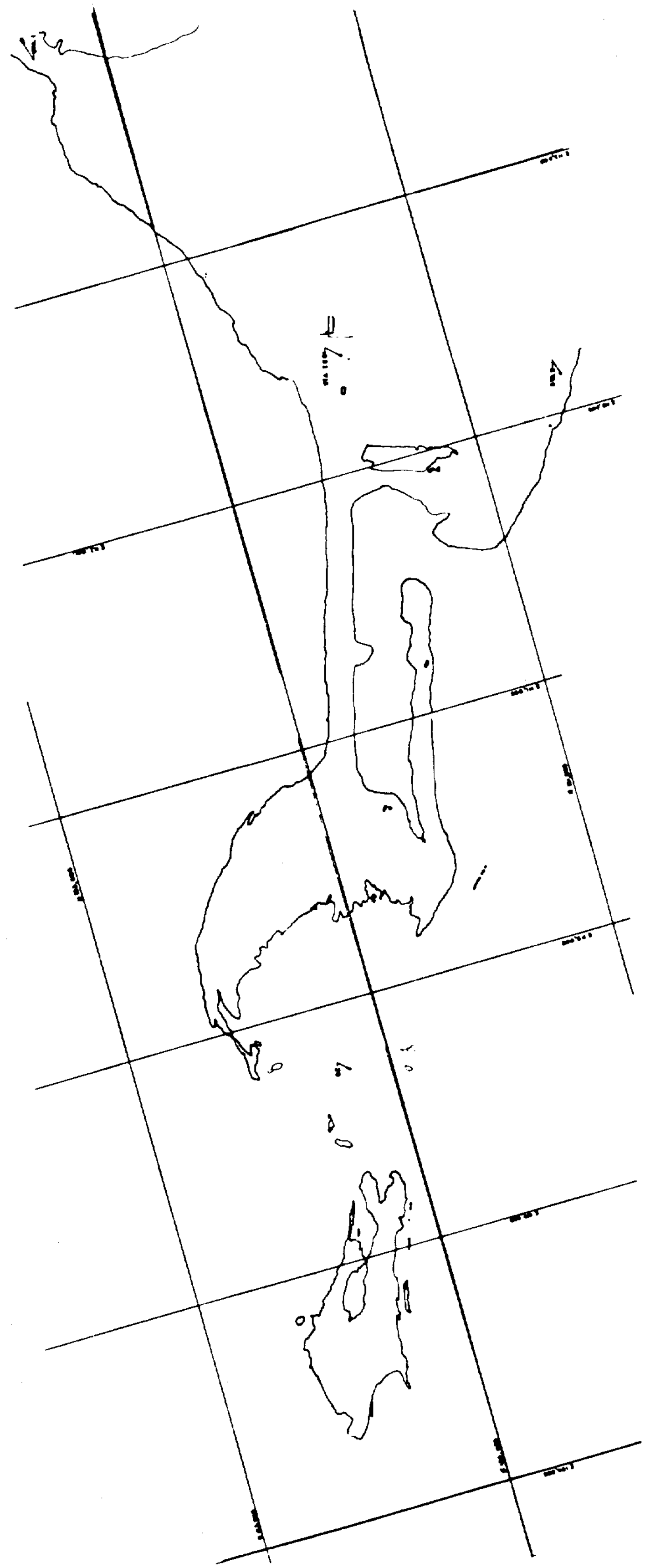

Figure 3.17 Mohawk stereophotogrammetric measurements.

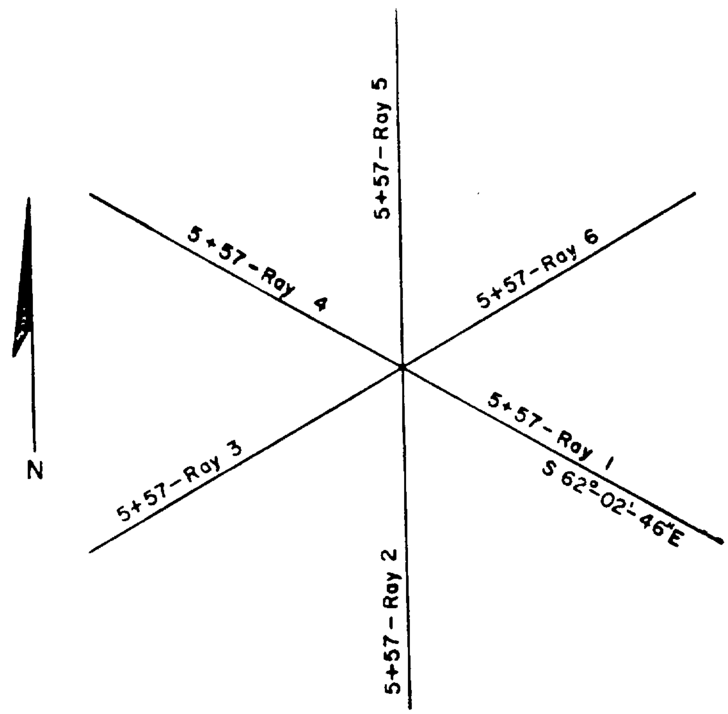

Figure 3.18 Mohawk survey lines.

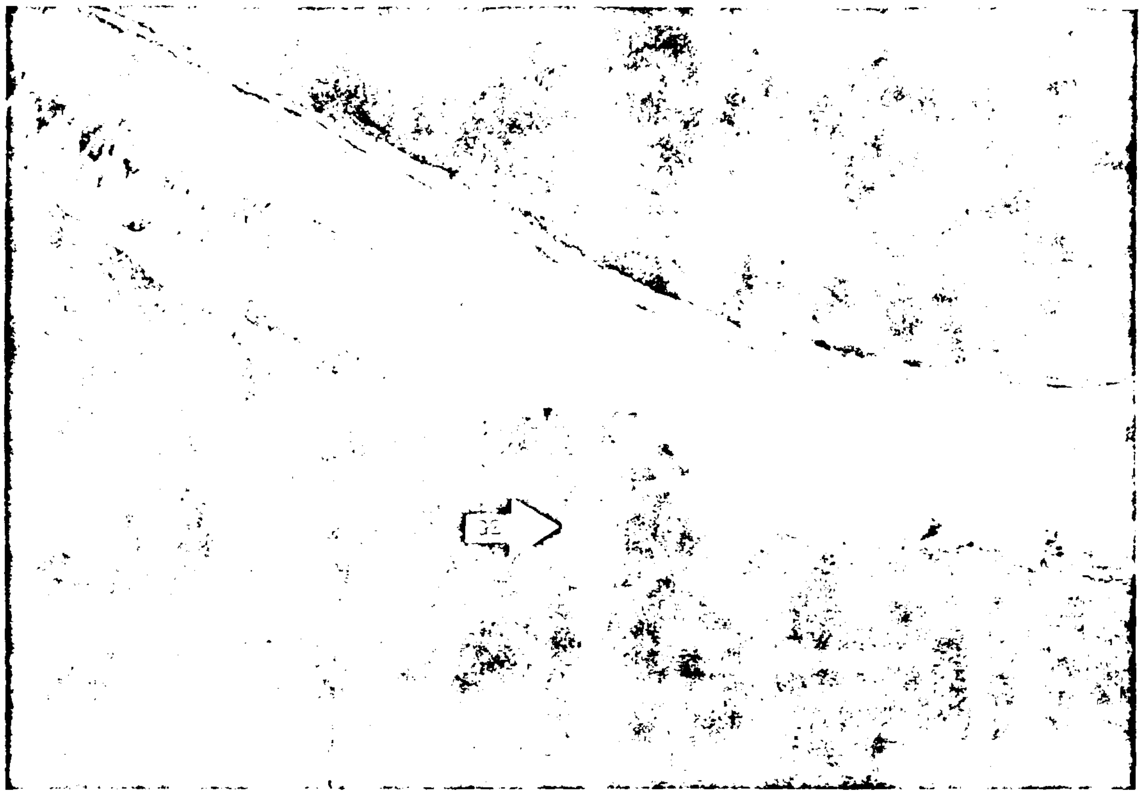

Figure 3.20 Tewa, postshot.

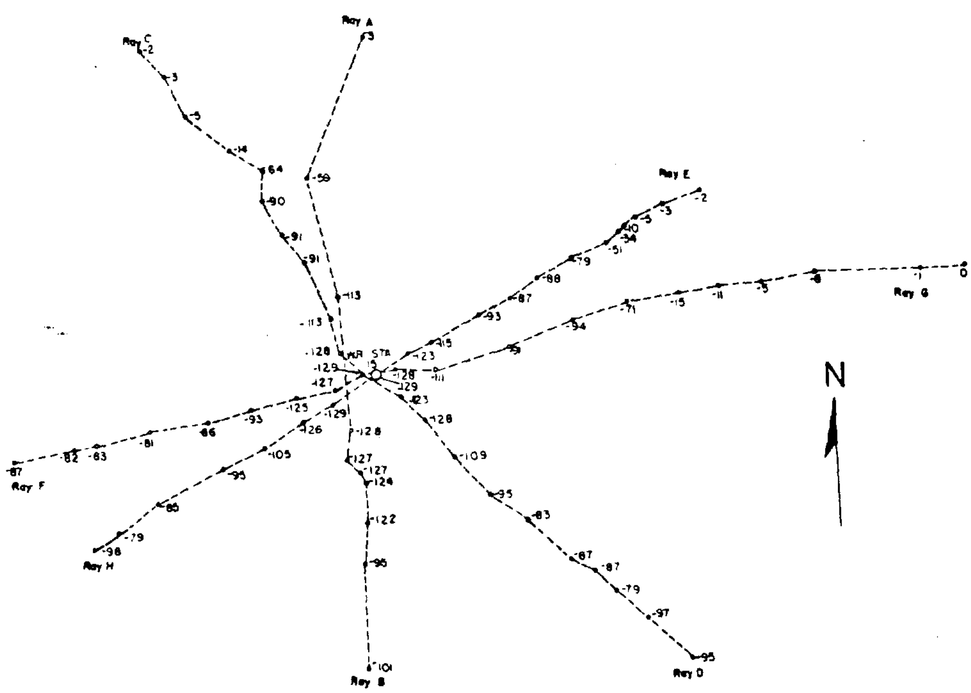

Figure 3.21 Tewa postshot survey rays.

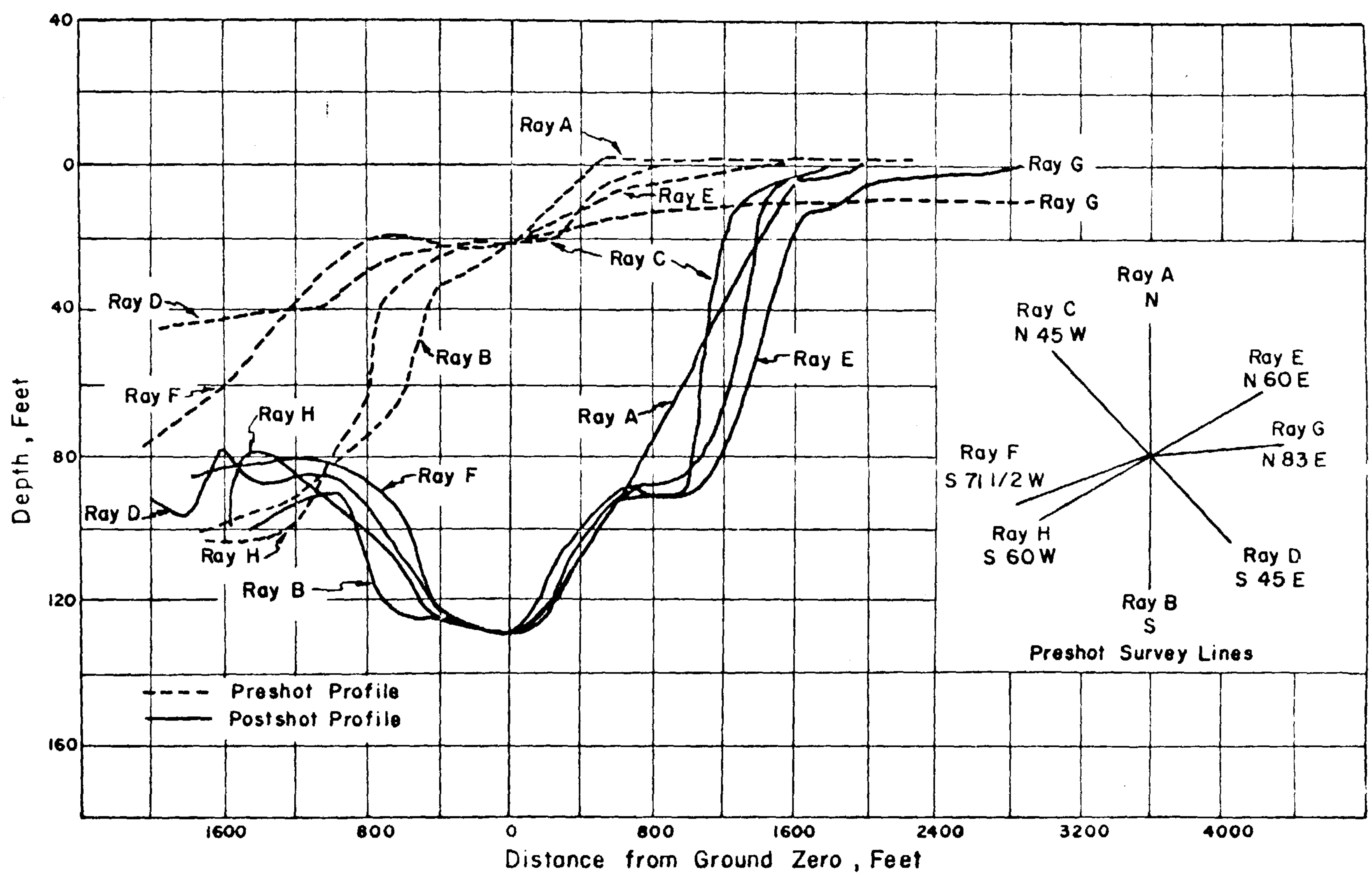

Figure 3.22 Tewa preshot and postshot profiles.

Chapter 4
DISCUSSION

In order to enhance the value of the discussion of the Redwing cratering results, a comparison should be made with crater measurements from other nuclear bursts in the Eniwetok Proving Ground. A summary of EPG cratering data is presented in Table 4.1. Crater radii, scaled to 1 kt, are plotted against height of burst on Figure 4.1. A similar plot of crater depths is made on Figure 4.2. Comparing these curves with the curves for dry soils from TM 23-200, it is apparent that some explanations are in order. The larger radii measured for the EPG craters may be attributed to soil factors (Reference 9), but it is felt that the washing action was an important contributing factor. This is also reflected in the fact that crater depths are less in the EPG. It appears that some peculiar burst configuration or environmental condition influenced the crater dimensions of Shots Lacrosse, Seminole, and Zuni to a marked degree. It should be re-emphasized here that only apparent or washed crater measurements were taken during Redwing as well as during all previous cratering bursts, both at NTS and at EPG, with one exception (Teapot Shot 7), for which true crater dimensions were taken. As defined in Section 1.3, the apparent crater is that deformation of the ground surface that is visible to the eye subsequent to the completion of the dynamic effects of the explosion. It should also be remembered that the majority of the craters measured in the Pacific had vented to open water and had undergone some degree of washing from waves created by the explosion. The alteration of the crater through washing action is believed to differ for each shot, and it is felt that the extent by which the waves generated by the explosion removed the material deposited in the crater lip is a rough measure of the degree of washing.

As mentioned earlier, soil type, energy partition, and height or depth of burst all play an important role in determining crater size and shape. The data from this project give good examples of these effects.

4.1 GEOLOGICAL STRUCTURE

Investigation of the geologic structure of Eniwetok were made by Scripps Institution of Oceanography and summarized by Porzel in Reference 1. Another investigation was made and the results published in the Bulletin of American Association of Petroleum Geologists in October 1953 (Reference 6). Since Bikini Atoll is similar in structure to Eniwetok, a brief summary of Eniwetok is felt to be sufficient (References 7 and 8).

The atoll consists of various layers of lenses of material interspersed with large cavities of water and air. With the exception of a few feet of hard rock at a depth of approximately 20 feet, the atoll is composed primarily of soft, unconsolidated sedimentary beds contained on the ocean side by a sheath of coral rock of varying thickness. This container wall is expected to have numerous weak spots because of joints and fissures characteristic of coral formations. At depths greater than 1,100 feet, hard or firm sedimentary layers become more prevalent and at a depth of 2,900, running up to 1,000 feet in thickness, the atoll is made up of a soft, chalky limestone. The atoll rests on a consolidated basalt floor, which is about 4,000 feet below sea level.

The excess density of the inner material that makes up the atoll over that of the water represents an enormous amount of potential energy by virtue of its elevation above the ocean floor. For this reason, it is considered to be in a metastable state contained by the structural strength of its coral jacket, by rock formations within the material, and by internal friction of the material formation (Reference 1).

4.2 SHOT LACROSSE

The Lacrosse crater presents an example of a relatively unwashed crater from a large-yield explosion. The crater lip (Figure 3.2) did not breach, showing that there was no rapid flow of water into and over the crater. There appears to be, however, some evidence of sloughing of the crater side, as shown by the profile (Figure 3.3). Scaled-wise, the crater was smaller in radius and greater in depth than EPG washed craters and

TABLE 4.1 EPG CRATER DATA

Shot	Weapon Yield	Burst Height	H_c-Scaled	Crater Radius	R_c-Scaled	Crater Depth	D_c-Scaled	R/D	Site
		H_c-ft	ft/kt$^{1/3}$	R_c-ft	ft/kt$^{1/3}$	D_c-ft	ft/kt$^{1/4}$		
Redwing									
Lacrosse	39.5 kt	17	5.00	202	59	44	17.6	—	Eniwetok
Zuni	3.53 Mt	9.25	0.61	1,155	76	103	13.4	11.2	Bikini
Seminole		-12 *						—	Eniwetok
Mohawk		300						—	Eniwetok
Tewa	5.01 Mt	20 *	1.17	2,000	117	129	15.7	16.8	Bikini
Greenhouse									
Dog		300					—	—	Eniwetok
Easy	46.7 kt	300	83.5	700	195	3	—	—	Eniwetok
George		200						—	Eniwetok
Ivy									
Ivy Mike	10.5 Mt	35	1.6	2,800	128	120	11.95	23.4	Eniwetok
Castle									
Castle No. 1	14.5 Mt	15.5	0.64	3,000	123	240	21.8	12.5	Bikini
Castle No. 3	110 kt	13.6	2.84	400	83.4	40	12.5	10	Bikini

* See discussion about burst height.

falls between the results expected for NTS soil and those expected for EPG soil. The Lacrosse crater also differed from other EPG craters in that the sides were steep and the bottom relatively flat. The steep sides of the crater are similar to those observed in craters formed in rock or concrete by high explosives. The flat bottom is also similar to those formed in hard rock or formed in material above a rock or concrete interface (Reference 10). In examining the shot site, it was found that Lacrosse was detonated over a large cemented platform, probably filled with coral, situated on a reef located at the northwest end of Site Yvonne. A drilling log, to the northeast of ground zero (made during Operation Hardtack) showed layers of hard cemented sand at 16 and 45 feet below the ground surface.

Since the Lacrosse crater is the first nuclear crater in saturated soil that did not breach to open water, it is to be expected that it will be compared to NTS craters by means of a soil factor. However, to obtain such a factor, it is necessary to compare the Lacrosse crater conditions with those of the standard dry-soil curves for NTS. In order to adjust the Lacrosse crater radius, it is necessary to apply a correction factor for hardness, since the Lacrosse site is harder and more rocklike than the NTS soil (which is considered to have a factor of 1) but not as hard as granite (for which a factor of 0.8 is given). If a factor of 0.9 is assumed and the radius adjusted for hardness and scaled to 1 kt, it is approximately 65.6 feet instead of 59 feet. The equivalent crater radius obtained from TM 23-200 is 45 feet, thereby making the soil factor, presumably due to moisture content, 1.46. This would tend to substantiate TM 23-200, which gives a factor of 1.5 for saturated soil. It is felt, however, that for media other than sand, such as coral or rock, the degree of saturation is lower and a smaller factor should be used. In the case of Lacrosse, a factor of 1.3 to 1.4 may be more applicable.

The adjusted crater depth is more a matter of conjecture, but it is felt that the underlying formations, acting as interfaces, decreased the depth considerably. The relative

flatness of the crater bottom tends to support this theory. It is believed that the crater depth would have about the same soil factor as the crater radius had no interfaces been present. A depth factor of 1.5 is given in TM 23-200 for saturated sand.

One shot is not considered sufficient evidence from which to obtain a soil factor, and one obtained from data such as given above is based at the best on a large amount of guesswork.

4.3 SHOT ZUNI

It is felt that the Zuni results should be viewed rather critically before being included in the weapon-effect literature because of the unusual burst situation. Ground zero for this burst was less than 100 feet from the edge of the water-filled Morgenstern crater. This may have affected the resulting crater. Since so much of the area encompassed by subsurface shock was underwater, the shock was transmitted through water for a considerable distance before entering the earth. It could be expected that water would not attenuate the shock as much as soil, thereby giving an abnormal effect on that side of ground zero. However, the shock strength could have been changed by reflection at the water-soil interface. The size of the crater is smaller than expected, both in radius and depth, and because of the many difficulties in explaining conditions surrounding the burst, it is not felt that this difference from the average EPG results should be considered serious.

An interesting aspect for conjecture on this shot is offered when the photographs (Figures 3.5 and 3.6) are compared with those of Mohawk (Figures 3.15 and 3.16). Although the heights of burst were quite different, Zuni being a near-surface burst and Mohawk a tower burst, the results were similar in that the crater removed the end of an island. The photographs show that Zuni tended to peel back the corners of the main island, whereas Mohawk did not.

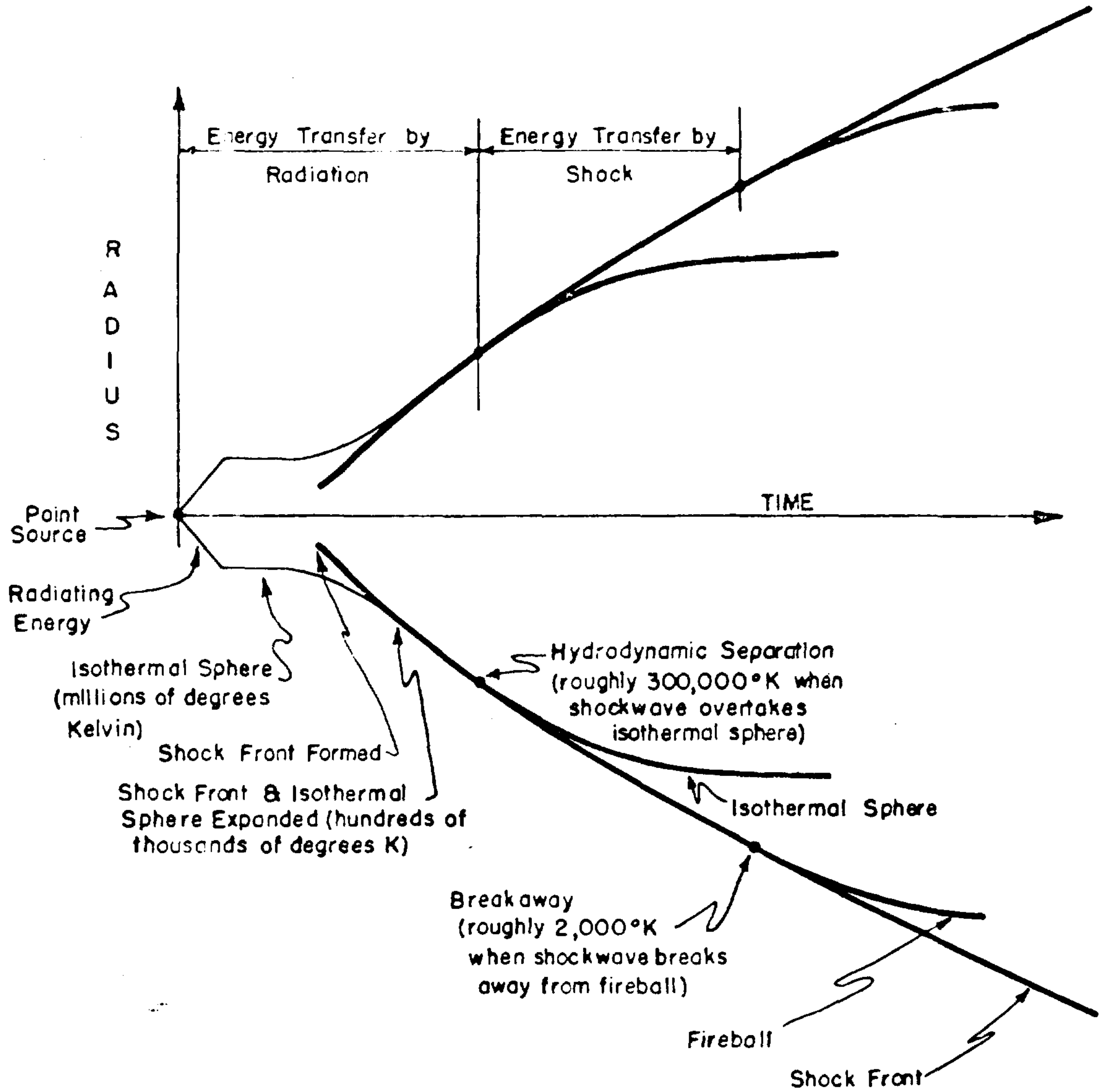

Figure 4.3 Early development of nuclear detonation.

Although there is no soil data available by which a comparison between the two sites could be made, there is a possibility that the soil in the center of the Zuni island had sufficient strength or was dry enough to reduce the Zuni crater radius toward the center of the island. However, it is felt that a more likely solution is that there was a narrower reef rim around the Zuni island than around the Mohawk island, as appears probable from the photographs. This would, of course, result in less support for the material in the rupture zone at the crater edge, a condition which would be aggravated by the larger yield and lower height of burst in the case of Shot Zuni. The resultant sloughing of the rupture zone would be encouraged by severe washing by the waves created by the explosion. Wave action at the Zuni site was severe enough to wash away all evidence of a lip if any existed. The Mohawk crater, on the other hand, does not seem to have undergone as severe washing, since the crater lip still exists.

4.4 SHOT SEMINOLE

The relationship of the burst point of this shot to the ground surface must be examined before the crater results are compared with previous data. The nuclear device was detonated inside a 50-foot-diameter tank of water, 25 feet deep, with the center of gravity of the charge 4.5 feet above the bottom of the tank (Figure 3.14). The least dimension to outside air in any direction was approximately 10 feet. This material should have provided sufficient mass to cause the temperature of the isothermal sphere to be reduced so that transfers of energy by shock would be faster than by radiation. This probably occurs at about 300,000 K (Figure 4.3). If we can assume that the isothermal sphere had proceeded into a shock phase before it reached the top of the water tank and that each cubic foot of water looks like about 0.6 cubic feet of earth during the radiative transport phase, then the energy partitioning of the burst may be similar to that for an underground burst with a charge depth of about 12 feet. For this reason, in reducing the crater dimensions, the crater depth is referenced to the adjusted surface of the water in the tank. The early growth of the isothermal sphere, when it is near an interface such as air and earth, plays a large part in determining the energy partition of the burst between the two media. Shot Seminole appears to be an excellent example of this. Further evidence of the effects of the water tank on energy partitioning is the fact that the radius was somewhat larger in the direction of the greatest thickness of water in the tank. This can be seen in Figure 3.12.

There is no information available on the depth of the water in the proximity of ground zero nor of the postshot crater in these areas, since all surveys were made along the lines indicated. However, it is felt that any effect on the crater due to these areas is minor in comparison to the effect caused by the water tank.

Again the existence of a lip may indicate the lack of complete washing, due probably to the protection offered the crater by the surrounding land mass. The crater radius then should probably be increased by 10 percent or more to be fully washed.

4.5 SHOT MOHAWK

This burst was on a 300-foot tower. The crater dimensions compare favorably with predictions, as evidenced in Figures 4.1 and 4.2, although the existence of a lip may indicate that full washing did not occur and the radius should be increased by 10 percent.

4.6 SHOT TEWA

This shot was fired on a barge in approximately 20 feet of water adjacent to the Charlie-Dog reef of Bikini Atoll. Although the bottom slopes from north to south through ground zero (Figures 3.20 and 3.22), this variation is small when compared to charge size. Due to the air-water and the water-ground interfaces, however, it is believed that less energy was channeled into cratering and the radius figure given is probably low. It is also difficult to assume a height of burst, but it is believed that it should be between 0 and 20 feet. This report uses 20 feet, which when scaled, should be close.

4.7 SUMMARY

The EPG operations from which cratering data are available are listed in Table 4.1. These data have been used to construct cratering curves for washed craters in saturated soil (Figures 4.1 and 4.2).

In Figure 4.1, the lower line is the dry-soil curve from TM 23-200 representing NTS conditions; the dotted line is the TM curve displaced by a factor of two in order to adjust for washing; the upper line is a curve drawn through data available from EPG. The EPG points are plotted from the data in Table 4.1, with the exception of dotted lines indicating possible limits of Seminole when adjusted as an underground burst and as an underground burst with washing. The Seminole adjustments have been made so that a trend line could be drawn for underground detonations.

The shots in which the crater radii do not fit the adjusted TM curve may be explained by the extreme difficulty in obtaining crater dimensions at EPG, especially for tower bursts or for large craters; an unwashed crater such as Lacrosse; different degrees of washing as in the case of Seminole, Mohawk, and Castle Shot 3 (the radius of these shots should be adjusted upward by at least 10 percent); or unusual environmental conditions, as in the case of Seminole, Zuni, or Castle Shot 3. The Seminole device was placed in a tank of water, part of the energy from Zuni vented into the lagoon, and Castle Shot 3 had radii listed at 380, 400, and in excess of 600 feet (the true radius is probably closer to 500 feet than the 400 feet commonly listed). If, for near-surface bursts, a soil factor should be derived for comparing the radius of the EPG washed craters in saturated coral to the Nevada cratering curve given in TM 23-200, a factor of 1.8 to 2.0 should be used. This factor is substantiated by a series of high-explosive surface charges fired on Eniwetok during Operation Ivy and compared to similar data gathered at NTS during the "Mole" experiment and Operation Jangle (References 3 and 9).

As more Pacific operations are conducted and additional cratering data is obtained, there is a trend apparent in the data from surface explosions. This trend is the increase in the ratio of the crater radius to crater depth as the yield increases into the multimegaton range. One would expect that as the yield and, correspondingly, the duration of the positive phase of the air blast gets very large, lower pressure would be required to produce measurable displacement at ground surface. This is because the impulse required to produce ground displacement sufficient to be measured as part of the crater can be obtained from lower pressures as the duration increases.

The crater depth data is not as consistent as the radius data and does not lend itself to soil factors, but should be accepted as a curve for approximate crater depths for air and surface bursts over saturated coral. As mentioned above, as the yield increases so does the value of R/D. This is due to the fact that depth does not increase at the same rate as radius. It is believed that this is caused by the increasing lack of similitude of the soil with increasing real depth as the yield increases. Simply stated, the hydrostatic forces at a point in soil 300 feet below the surface are much greater and different from those at a point 30 feet below the surface. Scale-wise, these are the same cube root scaled depths for a 1-kt and a 1-Mt device.

As can be realized from the above discussion, the larger the yield of weapon the greater the depth and, thus, the greater the deviation from cube-root scaling. This lack of scaling should apply to all soils and indicates the dangers in extrapolating present data on crater depth to extremely high yields. The use of higher root scaling will give closer approximations over a wider range; however, no scaling for depth will be absolutely accurate.

Chapter 5
CONCLUSIONS and RECOMMENDATIONS

5.1 CONCLUSIONS

The data obtained from these shots have increased the reliability of crater prediction for saturated soil types and washed craters. In addition, information has been obtained on an unwashed crater.

Underground shots are needed in order to extend the curves, or if the curves are extrapolated by soil factor to include underground bursts, they should be used with due caution.

There is no justification for modification of crater prediction curves in TM 23-200 for air and surface bursts in the regions of military significance.

5.2 RECOMMENDATIONS

Curves constructed in Figure 4.1 and 4.2 should be incorporated in the weapon-effect literature.

Future crater-producing bursts at the EPG should be closely monitored for cratering effects. .

REFERENCES

1. F. B. Porzel; "Ground-Shock Measurements: Crater Survey"; Annex 1.6, Part VI, Section 2, Operation Greenhouse, WT-109, December 1953; Los Alamos Scientific Laboratory, Los Alamos, New Mexico; Secret Restricted Data.

2. James L. Gaylord; "Photographic Crater Survey"; Project 3.7, Operation Ivy, WT-618, March 1953; Lookout Mountain Laboratory, Los Angeles, California; Unclassified.

3. R. B. Vaile; "Crater Survey"; Project 3.2, Operation Castle, WT-920, June 1955; Stanford Research Institute, Stanford, California; Secret Formerly Restricted Data.

4. D. T. Griggs; "Notes on Surface and Underground Bursts"; Project 1.9-2, Operation Jangle, WT-378, July 1952; Rand Corporation, Santa Monica, California; Unclassified.

5. "Craters Made by Ground Burst Nuclear Bombs"; FWE-17, U. S. Atomic Energy Commission, 30 July 1954; Confidential.

6. H. S. Ladd and others; "Drilling on Eniwetok Atoll, Marshall Islands"; The Bulletin of the American Association of Petroleum Geologists, Volume 37, Number 10, October 1953.

7. Dames and Moore Report; "Eniwetok Atoll"; 9 March 1951, and Supplement, 14 August 1953.

8. Dames and Moore Report; "Bikini Atoll"; 14 August 1953.

9. W. J. Christiansen, Jr.; "Cratering from Atomic Weapons"; AFSWP-514; Secret Restricted Data.

10. "Effects of a Soil-Rock Interface on Cratering"; Technical Report No. 2-478, May 1958; U. S. Army Engineer Waterways Experiment Station, Corps of Engineers, Vicksburg, Mississippi.